# Both Magnetic Resonance Imaging and Computed Tomography Are Reliable and Valid in Evaluating Cystic Osteochondral Lesions of the Talus

En Deng,* MD, Lixiang Gao,† MD, Weili Shi,* MD, Xing Xie,* MD, Yanfang Jiang,* MD, Huishu Yuan,†‡ MD, and Qinwei Guo,*‡ MD
*Investigation performed at the Institute of Sports Medicine, Peking University Third Hospital, Beijing, China*

**Background:** Compared with computed tomography (CT), magnetic resonance imaging (MRI) might overestimate the condition of osteochondral lesions of the talus (OLTs) owing to subchondral bone marrow edema and the overlying cartilage defect. However, no study has compared MRI and CT directly in evaluating OLTs with subchondral cysts.

**Purpose:** To compare the reliability and validity of MRI and CT in evaluating OLTs with subchondral cysts.

**Study Design:** Cohort study (diagnosis); Level of evidence, 2.

**Methods:** An institutional radiology database was queried for inpatients diagnosed with OLTs with subchondral cysts who had undergone surgical treatment between May 2015 and October 2019. A total of 48 patients met the inclusion criteria. Based on our measurement method, 2 experienced observers who were blinded to the study independently measured the length, width, and depth of the cysts using MRI and CT. The classification of cystic lesions was also performed based on MRI and CT findings.

**Results:** Interobserver reliability was almost perfect, with intraclass correlation coefficients (ICCs) ranging from 0.935 to 0.999. ICCs for intraobserver reliability ranged from 0.944 to 0.976. The mean size of cysts measured on MRI (length, $13.38 \pm 4.23$ mm; width, $9.28 \pm 2.28$ mm; depth, $11.54 \pm 3.69$ mm) was not significantly different to that evaluated on CT (length, $13.40 \pm 4.08$ mm; width, $9.25 \pm 2.34$ mm; depth, $11.32 \pm 3.54$ mm). The size of subchondral cysts was precisely estimated on both MRI and CT. The MRI classification and CT classification revealed almost perfect agreement (kappa = 0.831).

**Conclusion:** With our measurement method, both MRI and CT were deemed to be reliable and valid in evaluating the size of subchondral cysts of OLTs, and the MRI classification was well-correlated with the CT classification. The presented measurement method and classification systems could provide more accurate information before surgery.

**Keywords:** osteochondral lesion; talus; cysts; measurement

Osteochondral lesions of the talus (OLTs) are being recognized as increasingly common injuries,[20] occurring in up to 50% of acute ankle sprains, chronic ligament instability, and fractures.[23,30] They mainly affect young, sports-active patients.[12] The lesions involve articular cartilage and/or subchondral bone, causing deep chronic ankle pain, swelling, stiffness, weakness, giving way, blocking of the joint, a reduction of sports activity and quality of life, and eventually, osteoarthritis.[9,11,12]

Previous studies show that OLTs respond poorly to nonsurgical treatment[24,28] and require arthroscopic or nonarthroscopic bone marrow stimulation, with reported

satisfactory success rates.[5,13,21] Shimozono et al[25] found that subchondral cysts had a negative impact on clinical scores after surgery. Although OLTs with small cysts (<8 mm) can be treated effectively with microfracture or abrasion arthroplasty, lesions with a large subchondral cyst may require replacement techniques.[6,7,22,31] Thus, the size of the subchondral cyst plays an important role in postoperative clinical outcomes and decision making during surgery for cystic OLTs.

With routine radiography, which has long been the first choice for diagnostic imaging, up to 50% of OLTs of the ankle may be missed.[14,20] More recently, to better evaluate the condition of OLTs, magnetic resonance imaging (MRI) and computed tomography (CT) have been used.[3,16,18] CT can provide more precise information than MRI on subchondral bone, such as the size, the shape, bone sclerosis,

absorption, the subchondral bone plate (SBP), and cysts.[18] In contrast, with its exceptional resolution and high signal-to-noise ratio, MRI has been accepted as the standard imaging tool with excellent sensitivity and specificity in evaluating cartilage, soft tissue, and subchondral bone, such as subchondral bone marrow edema (BME) and cysts, without exposure to radiation.[19,27] Nevertheless, CT has been deemed to be a precise imaging modality in evaluating the dimensions of OLTs,[2] and several studies have reported that MRI might overestimate the condition of the lesions owing to BME and the overlying cartilage defect.[10,15] No study, to the best of our knowledge, has compared MRI and CT directly in evaluating subchondral cysts of OLTs.

The primary purpose of this retrospective study was to investigate the reliability and validity of MRI compared with CT in evaluating cystic OLTs. We hypothesized that MRI would be reliable and valid compared with CT in measuring subchondral cysts of OLTs and that MRI would be as useful as CT in facilitating decision making during surgery.

## METHODS

### Patients

Patients who visited the sports medicine clinic of our department for the diagnosis of OLTs between May 2015 and October 2019 were retrospectively evaluated in the present study. The inclusion criteria were as follows: (1) patients who preoperatively underwent both CT and MRI on the same day and had confirmed OLTs, for which they then underwent surgical treatment; (2) a lack of response to at least 3 months of nonoperative treatment; and (3) the presence of a subchondral cyst with a diameter larger than 8 mm. Patients with previous ankle surgery were excluded from this study. The diagnosis of OLT was based on medical history, physical examination results, and imaging findings. The diameter of the cyst was determined by averaging the maximum diameters of the cyst on coronal, sagittal, and axial CT and MRI. All patients were assessed by the first author (E.D.). All participants signed informed consent forms. The current study was approved by the local ethical committee of the hospital.

### CT Evaluation

CT scans in the coronal, sagittal, and axial planes were obtained with a multichannel CT scanner (Siemens). The patient was placed in a supine, neutral position. The scan

parameters included a $512 \times 512$ matrix, 3-mm slice thickness, 8.86 ms scan time, 1.0-second rotation time, 100 kV, and 150 mAs.

### MRI Evaluation

MRI scans were obtained using a Signa HDxt 3.0-T device (GE Healthcare) with an 8-channel ankle joint surface coil. Proton density spin echo scans in the coronal, sagittal, and axial planes were collected. The parameters for the coronal planes were as follows: repetition time, 2780 milliseconds; echo time, 38 milliseconds; and section thickness, 2.5 mm. Those for the sagittal planes were as follows: repetition time, 2120 milliseconds; echo time, 38 milliseconds; and section thickness, 3 mm. Those for the axial planes were as follows: repetition time, 2600 milliseconds; echo time, 36 milliseconds; and section thickness, 3 mm. The field of view was $16 \times 16$ cm.

### Measurement of Cysts

There were 2 experienced observers (L.G., E.D.), blinded to the present study, who performed the measurements independently. Moreover, a standard picture archiving and communication system (PACS) viewing station was used. Both observers measured the cysts twice on every patient, with an interval of 2 months between measurements, to evaluate intraobserver reliability. These 2 observers were blinded to the measurements made by each other and their own first measurement. In addition, the images were anonymized and randomly sorted.

The largest diameters of the cyst on the coronal, sagittal, and axial CT and MRI images were measured, which were defined and determined as follows. On the coronal image, a tangent along the lowest point of the talus dome was drawn to measure the width and depth of the bone cyst (parallel and perpendicular to the tangent). On the sagittal image, a tangent along the talus dome was drawn to measure the length and depth of the bone cyst (parallel and perpendicular to the tangent). On the axial image, a tangent along the midpoint of the left and right sides of the talus was drawn to measure the width and length of the bone cyst (parallel and perpendicular to the tangent) (Figure 1). The diameter of the cyst for each patient was determined from the maximum length, width, and depth measured above. The ratio of the largest area of subchondral BME to the talus was measured on the sagittal image of T2 weighted imaging MRI: ratio = (*maximum transverse diameter* ×

‡Address correspondence to Qinwei Guo, MD, Institute of Sports Medicine, Peking University Third Hospital, 49 North Garden Road, Haidian District, Beijing 100191, China (email: guoqinwei@vip.sina.com); and Huishu Yuan, MD, Department of Radiology, Peking University Third Hospital, 49 North Garden Road, Haidian District, Beijing 100191, China (email: huishuy@sina.com).

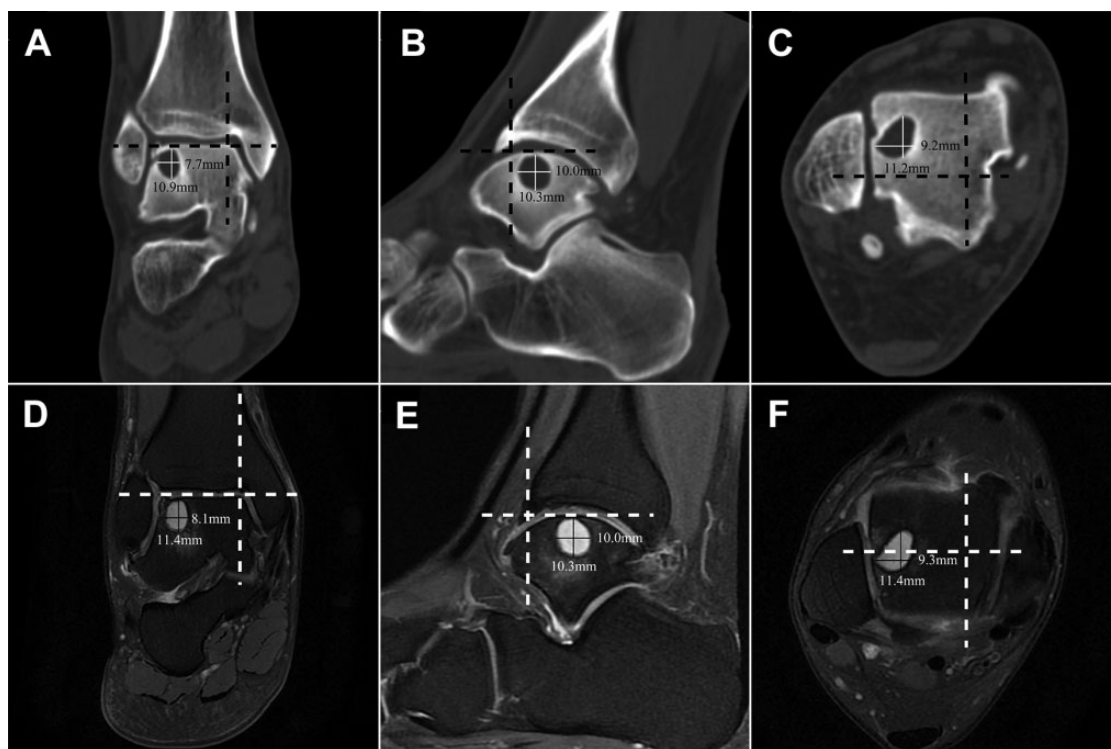*Institute of Sports Medicine, Peking University Third Hospital, Beijing, China.

†Department of Radiology, Peking University Third Hospital, Beijing, China.

E.D. and L.G. contributed equally to this article.

**Figure 1.** Diameter measurement on computed tomography (CT) and magnetic resonance imaging (MRI): (A) coronal CT, (B) sagittal CT, (C) axial CT, (D) coronal MRI, (E) sagittal MRI, and (F) axial MRI. In this case, the maximum length, width, and depth of the cyst on CT were 11.2, 9.2, and 10.9 mm, respectively, and those on MRI were 11.4, 9.3, and 11.4 mm, respectively.

*vertical diameter of edema)/(maximum transverse diameter × vertical diameter of talus).*

The cysts were classified into 3 types on CT scans according to Nakasa et al[16]: type I, irregular shape; type II, rounded shape with hardened walls; and type III, open to the articular surface. In the present study, a classification system was developed to divide cysts on MRI scans into 3 types according to BME and the SBP: type I, a complete SBP and BME larger than 50% of the talus area; type II, a complete SBP and BME smaller than 50% of the talus area; and type III, an incomplete SBP (Figure 2).

## Statistical Analysis

All analyses were performed using SPSS Version 24.0 (IBM). Numerical variables were reported as the mean ± SD, such as the length, width, and depth of cysts of OLTs. All the measurements of the diameter of cystic OLTs were compared using intraclass correlation coefficients (ICCs) for interobserver and intraobserver reliability. Additionally, the kappa statistic was used to evaluate the consistency of the classification made by CT and MRI findings. An ICC or kappa that ranged from 0.81 to 1.00 was defined as almost perfect reliability, 0.61 to 0.80 as substantial, 0.41 to 0.60 as moderate, 0.21 to 0.40 as fair, and 0.00 to 0.20 as slight.[8] The paired-samples $t$ test was used for comparing the length, width, and depth of the cysts as measured between CT and MRI. A $P$ value $<.05$ was considered statistically significant.

## RESULTS

### Patient Demographics

In this retrospective study, a total of 48 patients (18 left ankles/30 right ankles) who met the inclusion criteria were included. They had a mean age of 42.63 ± 11.14 years (range, 20-63 years), and there were 36 (75%) male and 12 (25%) female patients.

### Interobserver and Intraobserver Reliability

Almost perfect interobserver reliability between two observers was achieved (0.935 ≤ ICC ≤ 0.999) (Table 1). The ICCs of the formal measurements of the 48 cases indicated almost perfect intraoberserver reliability (Table 1).

### Validity (Difference Between Modalities)

Mean results of the measurements were as follows: length, 13.38 ± 4.23 mm on MRI versus 13.40 ± 4.08 mm on CT ($t = -0.209; P = .836$); width, 9.28 ± 2.28 mm on MRI versus 9.25 ± 2.34 mm on CT ($t = 0.373; P = .711$); and depth, 11.54 ± 3.69 mm on MRI versus 11.32 ± 3.54 mm on CT ($t = 1.446; P = .155$). The mean length, width, and depth as measured in our study indicated no significant difference between MRI and CT.
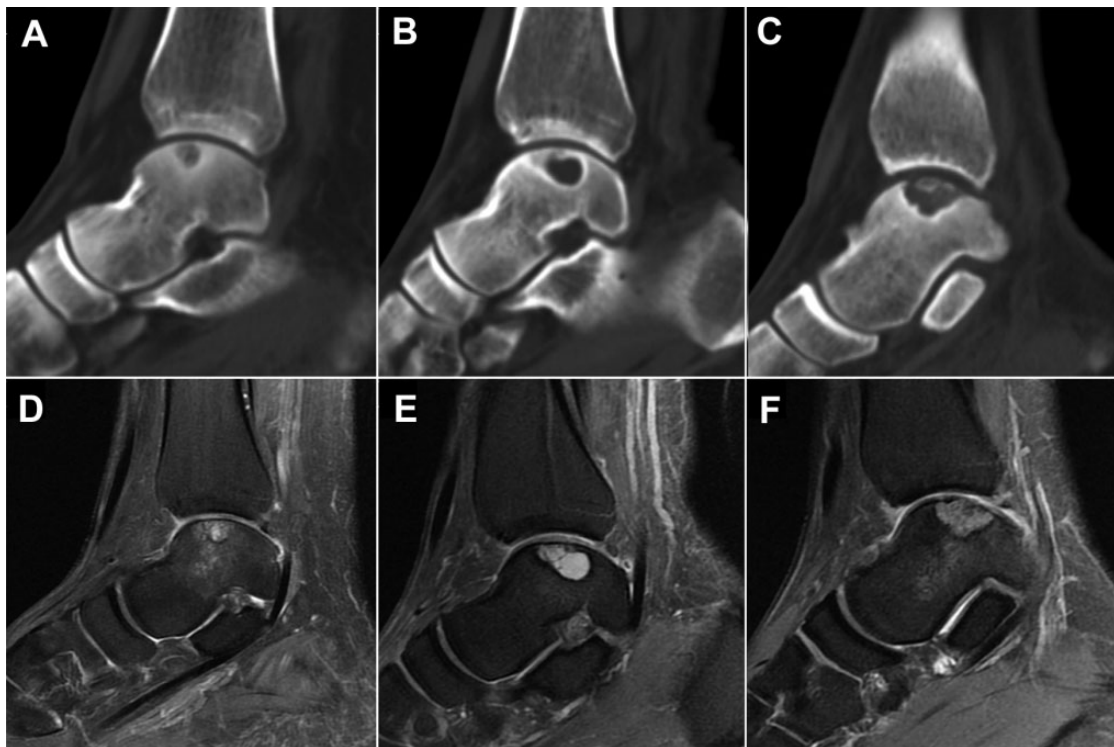
**Figure 2.** The cysts were classified into 3 types on computed tomography (CT): (A) Type I, (B) Type II, (C) Type III, and magnetic resonance imaging (MRI): (D) Type I, (E) Type II, (F) Type III, respectively.

TABLE 1
Interobserver and Intraobserver Reliability (ICC)[a]

|  | Interobserver | | Intraobserver |
|---|---|---|---|
|  | Observer 1 | Observer 2 | |
| MRI | | | |
| Length | 0.980 | 0.999 | 0.976 |
| Width | 0.935 | 0.997 | 0.944 |
| Depth | 0.957 | 0.999 | 0.965 |
| CT | | | |
| Length | 0.969 | 0.999 | 0.974 |
| Width | 0.939 | 0.998 | 0.964 |
| Depth | 0.975 | 0.998 | 0.965 |

[a]CT, computed tomography; ICC, intraclass correlation coefficient; MRI, magnetic resonance imaging.

TABLE 2
Classification of CT and MRI Findings[a]

|  | MRI | | | |
|---|---|---|---|---|
|  | Type I | Type II | Type III | Total |
| CT | | | | |
| Type I | 11 | 0 | 1 | 12 |
| Type II | 1 | 23 | 3 | 27 |
| Type III | 0 | 0 | 9 | 9 |
| Total | 12 | 23 | 13 | 48 |

[a]Data are presented as No. CT, computed tomography; MRI, magnetic resonance imaging.

## Classification of CT and MRI Findings

As shown in Table 2, the classification of CT findings was as follows: type I, 12 patients (25.0%); type II, 27 patients (56.3%); and type III, 9 patients (18.7%). The classification of MRI findings was as follows: type I, 12 patients (25.0%); type II, 23 patients (47.9%); and type III, 13 patients (27.1%). MRI type I lesions consisted of 11 cases (11/12; 91.7%) of CT type I and 1 case (1/12; 8.3%) of CT type II. All ankles with MRI type II (23/23; 100.0%) revealed CT type II. MRI type III lesions consisted of 1 case (1/13; 7.7%) of CT type I, 3 cases

(3/13; 23.1%) of CT type II, and 9 cases (9/13; 69.2%) of CT type III. Comparing the MRI classification with the CT classification, the kappa statistic revealed almost perfect correlation between the 2 classifications, with a kappa of 0.831.

## DISCUSSION

The current research showed that both MRI and CT are deemed to be reliable and valid in evaluating the size of subchondral cysts of OLTs, with our measurement method, and that the MRI classification correlated well with the CT classification.

## Measurement Methods

In 2009, Choi et al[1] first defined a measurement method for OLTs: coronal length (horizontal extension measured from the coronal image), sagittal length (horizontal extension measured from the sagittal image), and depth (vertical extension measured from the sagittal image). Walley et al[29] suggested a new measurement method to estimate the true volume of OLTs using 3-dimensionally reconstructed images and volume analysis: lengths $w$ and $h$ (2 orthogonal axes that comprised the largest cross section of the OLTs on the sagittal image) and length $d$ (the largest diameter of the OLTs on the axial image). In some studies, the width was measured on the axial view, depth on the coronal view, and length on the sagittal view.[7,22] However, in the CT and MRI scans of the present study, the length, width, and depth measurements were performed on the axial, coronal, and sagittal views, respectively. Baseline measurements were determined by anatomic landmarks instead of horizontal and vertical lines, which may help to rule out the measuring errors caused by the different scanning positions of the ankle between different patients. In previous studies, with replacement techniques for OLTs with large subchondral cysts, such as autologous osteoperiosteal cylinder and osteochondral graft transplantation, the graft was harvested by a harvester tube that was perpendicular to the surface of the talus.[6,7,22,31] Therefore, compared with previous studies, our measurement method evaluated cysts in parallel and perpendicular to the tangent along the talus dome, obtaining a more precise dimension of graft transplantation preoperatively, which could provide more accurate information for surgery.

## Reliability and Validity

The ICCs revealed almost perfect interobserver and intraobserver agreement ($0.935 \sim 0.999$), indicating that both MRI and CT, with the presented measurement method, were reliable in measuring the cysts of OLTs. In our study, only subchondral cysts were assessed, without measurements of the cartilage defect. As CT can sensitively discriminate between bone and cysts, it has been an especially effective imaging modality for evaluating cysts in previous studies.[2] Previous studies have also reported that MRI might overestimate the condition of the lesions owing to BME and the overlying cartilage defect.[10,15] However, in this study, MRI was performed using a Signa HDxt 3.0-T device with an 8-channel ankle joint surface coil. Thus, with better sensitivity and specificity in discriminating between bone and soft tissue, the BME signal on our MRI scans was differentiated from that of the OLT cysts, which may have helped us to avoid overestimating subchondral cysts.

Each pixel on CT represents the average CT value of all components in the corresponding unit, which may not accurately show the CT value of various components in the unit. The CT value of lesions smaller than the thickness of the layer is affected by other tissue within the thickness of the layer, and the measured CT value cannot represent the true CT value of the lesion. On the contrary, the CT value of

smaller high-density lesions in low-density tissue is relatively low, which is called the partial-volume effect (PVE). Based on similar principles, the PVE also affects the measurement results on MRI. Soret et al[26] suggested that compensation for the PVE should account for both the finite resolution effect and the tissue fraction effect, and image sampling is one of the reasons for PVE. Nevertheless, section thickness, related to the PVE, is 2.5 or 3.0 mm on MRI, similar to that on CT, which means that interference of the PVE to MRI and CT is similar, and evaluating cysts on MRI might be as valid as on CT. In this study, MRI measurements of the length, width, and depth of cysts of OLTs were not significantly different from those on CT.

## Classification of CT and MRI Findings

In the pathogenesis of lesions in the subchondral region of OLTs, the importance of subchondral bone has been well discussed.[16] In addition, when classified according to the condition of subchondral bone on CT, there is a correlation between cartilage injuries and subchondral bone, and CT findings have correlated closely with arthroscopic findings compared with MRI.[16] Based on the condition of subchondral bone correlating with cartilage damage and the stability of lesions, CT therefore reinforces MRI capabilities, results in a precise diagnosis for OLTs, and is a useful tool for predicting cartilage injuries.[16,18] In the current study, MRI findings that were classified according to BME and SBP conditions correlated well with the CT classification (kappa = 0.831), which indicates that MRIs can predict precise information on subchondral bone, including the SBP and BME.

OLTs with a round shape and sclerotic wall cysts indicate that pressurized fluid no longer flows into the cysts, and bone remodeling occurs. Lesions do not increase, and damage of articular cartilage maintains in a relative low grade.[16] When trauma causes damage to cartilage and the SBP, continuous high-pressure liquid flows into subchondral bone, which induces osteolysis and subchondral cysts.[4,16] BME is characterized as an excessive fluid signal in subchondral bone on MRI,[12,27] and a sclerotic wall could limit the progression of BME.[19] Nakasa et al[17] reported that a large area of BME on MRI exhibited low degeneration of cartilage of the osteochondral fragment, while a small area of BME indicated sclerosis of subchondral bone with severe degeneration of cartilage. This means that the extent of BME on MRI could reflect cartilage degeneration. Additionally, a damaged SBP, especially disruption of the SBP, no longer maintains cartilage metabolism, which subsequently results in severe cartilage degeneration and articular damage.[16] An irregular shape cyst with an opening to the articular cavity indicates damaged SBP. Incomplete bone cortex according to the CT classification of Nakasa, is similar to MRI type III, which demonstrates a discontinuous signal of the SBP. Therefore, the MRI classification system developed in this study could reflect the condition of articular cartilage degeneration and the process of lesions, which may play an important role in surgical decision making and in prediction of the clinical outcomes of treatment.

## Limitations

This study is not without weaknesses, as it is a retrospective analysis in nature. However, all eligible patients were included in our study for analysis; thus, the number of patients included was not based on sample size calculation but on practicality. We did not observe a significant difference between MRI- and CT-based evaluations, perhaps because the outcomes were not sensitive, or too few patients were studied. Hence, a prospective database study with a larger sample size would likely provide better results. The findings were validated for a 3.0-T MRI machine, and lower (or higher) resolution MRI machines may have different findings. In our previous study,[7] a complete cyst was difficult to be harvested during surgery; thus, cyst size could not be assessed at surgery. In addition, arthroscopic examinations were not performed in some cases; therefore, we only compared the MRI classification with the CT classification, without correlating with arthroscopic findings or staging.

## Clinical Significance

Previous studies have suggested that CT is an especially effective tool in evaluating cysts of OLTs. This study showed that MRI is also reliable and valid in evaluating the size of subchondral cysts of OLTs compared with CT. In addition, MRI could be beneficial and safe for those who are incapable of undergoing CT, and the presented measurement method could provide more accurate information for surgery. Thus, we recommend MRI for diagnosing and evaluating OLTs with cysts.

## CONCLUSION

With our measurement method, both MRI and CT are deemed to be reliable and valid in evaluating the size of subchondral cysts of OLTs, and the MRI classification correlated well to the CT classification. The presented measurement method and classification systems could provide more accurate information for surgery.

## ACKNOWLEDGMENT

## REFERENCES

1. Choi WJ, Park KK, Kim BS, Lee JW. Osteochondral lesion of the talus: is there a critical defect size for poor outcome? *Am J Sports Med*. 2009;37:1974-1980.
2. Easley ME, Latt LD, Santangelo JR, et al. Osteochondral lesions of the talus. *J Am Acad Orthop Surg*. 2010;18:616-630.
3. Elias I, Zoga AC, Morrison WB, et al. Osteochondral lesions of the talus: localization and morphologic data from 424 patients using a novel anatomical grid scheme. *Foot Ankle Int*. 2007;28:154-161.
4. Giannini S, Vannini F. Operative treatment of osteochondral lesions of the talar dome: current concepts review. *Foot Ankle Int*. 2004;25: 168-175.
5. Guo QW, Hu YL, Jiao C, Yu CL, Ao YF. Arthroscopic treatment for osteochondral lesions of the talus: analysis of outcome predictors. *Chin Med J*. 2010;123:296-300.
6. Han SH, Lee JW, Lee DY, Kang ES. Radiographic changes and clinical results of osteochondral defects of the talus with and without subchondral cysts. *Foot Ankle Int*. 2006;27:1109-1114.
7. Hu Y, Guo Q, Jiao C, et al. Treatment of large cystic medial osteochondral lesions of the talus with autologous osteoperiosteal cylinder grafts. *Arthroscopy*. 2013;29:1372-1379.
8. Landis JR, Koch GG. The measurement of observer agreement for categorical data. *Biometrics*. 1977;33:159-174.
9. Lee KB, Bai LB, Chung JY, Seon JK. Arthroscopic microfracture for osteochondral lesions of the talus. *Knee Surg Sports Traumatol Arthrosc*. 2010;18:247-253.
10. Lee KB, Bai LB, Park JG, Yoon TR. A comparison of arthroscopic and MRI findings in staging of osteochondral lesions of the talus. *Knee Surg Sports Traumatol Arthrosc*. 2008;16:1047-1051.
11. Lee KB, Bai LB, Yoon TR, Jung ST, Seon JK. Second-look arthroscopic findings and clinical outcomes after microfracture for osteochondral lesions of the talus. *Am J Sports Med*. 2009;37(suppl 1): 63S-70S.
12. Leumann A, Valderrabano V, Plaass C, et al. A novel imaging method for osteochondral lesions of the talus: comparison of SPECT-CT with MRI. *Am J Sports Med*. 2011;39:1095-1101.
13. Li H, Hua Y, Li H, et al. Treatment of talus osteochondral defects in chronic lateral unstable ankles: small-sized lateral chondral lesions had good clinical outcomes. *Knee Surg Sports Traumatol Arthrosc*. 2018;26:2116-2122.
14. Loomer R, Fisher C, Lloyd-Smith R, Sisler J, Cooney T. Osteochondral lesions of the talus. *Am J Sports Med*. 1993;21:13-19.
15. Mintz DN, Tashjian GS, Connell DA, et al. Osteochondral lesions of the talus: a new magnetic resonance grading system with arthroscopic correlation. *Arthroscopy*. 2003;19:353-359.
16. Nakasa T, Adachi N, Kato T, Ochi M. Appearance of subchondral bone in computed tomography is related to cartilage damage in osteochondral lesions of the talar dome. *Foot Ankle Int*. 2014;35: 600-606.
17. Nakasa T, Ikuta Y, Sawa M, et al. Relationship between bone marrow lesions on MRI and cartilage degeneration in osteochondral lesions of the talar dome. *Foot Ankle Int*. 2018;39:908-915.
18. Nakasa T, Ikuta Y, Yoshikawa M, et al. Added value of preoperative computed tomography for determining cartilage degeneration in patients with osteochondral lesions of the talar dome. *Am J Sports Med*. 2018;46:208-216.
19. Nathan M, Mohan H, Vijayanathan S, Fogelman I, Gnanasegaran G. The role of 99mTc-diphosphonate bone SPECT/CT in the ankle and foot. *Nucl Med Commun*. 2012;33:799-807.
20. O'Loughlin PF, Heyworth BE, Kennedy JG. Current concepts in the diagnosis and treatment of osteochondral lesions of the ankle. *Am J Sports Med*. 2010;38:392-404.
21. Ramponi L, Yasui Y, Murawski CD, et al. Lesion size is a predictor of clinical outcomes after bone marrow stimulation for osteochondral lesions of the talus: a systematic review. *Am J Sports Med*. 2017; 45:1698-1705.
22. Sawa M, Nakasa T, Ikuta Y, et al. Outcome of autologous bone grafting with preservation of articular cartilage to treat osteochondral lesions of the talus with large associated subchondral cysts. *Bone Joint J*. 2018;100:590-595.
23. Saxena A, Eakin C. Articular talar injuries in athletes: results of microfracture and autogenous bone graft. *Am J Sports Med*. 2007;35: 1680-1687.
24. Shearer C, Loomer R, Clement D. Nonoperatively managed stage 5 osteochondral talar lesions. *Foot Ankle Int*. 2002;23:651-654.
25. Shimozono Y, Coale M, Yasui Y, et al. Subchondral bone degradation after microfracture for osteochondral lesions of the talus: an MRI analysis. *Am J Sports Med*. 2018;46:642-648.

26. Soret M, Bacharach SL, Buvat I. Partial-volume effect in PET tumor imaging. *J Nucl Med*. 2007;48:932-945.

27. Tamam C, Tamam MO, Yildirim D, Mulazimoglu M. Diagnostic value of single-photon emission computed tomography combined with computed tomography in relation to MRI on osteochondral lesions of the talus. *Nucl Med Commun*. 2015;36:808-814.

28. Verhagen RA, Struijs PA, Bossuyt PM, van Dijk CN. Systematic review of treatment strategies for osteochondral defects of the talar dome. *Foot Ankle Clin*. 2003;8:233-242.

29. Walley KC, Gonzalez TA, Callahan R, et al. The role of 3D reconstruction true-volume analysis in osteochondral lesions of the talus: a case series. *Foot Ankle Int*. 2018;39:1113-1119.

30. Waterman BR, Belmont PJ, Cameron KL, DeBerardino TM, Owens BD. Epidemiology of ankle sprain at the United States Military Academy. *Am J Sports Med*. 2010;38:797-803.

31. Zhu Y, Xu XY. Osteochondral autograft transfer combined with cancellous allografts for large cystic osteochondral defect of the talus. *Foot Ankle Int*. 2016;37:1113-1118.